



Anti-Rollover Warning Control of Dump Truck Lifting Operation Based on Active Suspension

Quguang Guan¹ · Aihong Gong¹ · Mingmao Hu¹ · Ziwen Liao¹ · Xin Chen¹

Received: 9 June 2020 / Revised: 20 September 2020 / Accepted: 29 October 2020 / Published online: 23 November 2020
© Brazilian Society for Automatics--SBA 2020

Abstract

The flexible parts of the dump truck such as the suspension, tires and cargo box can affect the roll stability of the vehicle during the lifting process. In order to improve the adverse effects of these flexible parts on the roll stability of the dump truck during lifting, and to prevent the vehicle from rolling over, this paper proposes an anti-rollover warning control method based on active suspension. The nonlinear model of the lift and roll of the dump truck is established by considering the influence of elastic deformation of the tire, suspension, and torsional deformation of the cargo box on the roll of the vehicle, and dynamic characteristics of the nonlinear model are verified in the MATLAB/Simulink simulation environment. A fuzzy-PID controller is designed to make decisions on the active suspension control force as well as the ratio of the vertical load of the non-bearing wheel to the total weight of the vehicle is used as the rollover evaluation index to realize the rollover warning. Furthermore, the improvement effect of the control system is analyzed from the aspects of rollover evaluation index, roll angle and critical lifting angle. Finally, the simulation results show that the proposed method effectively improves the roll stability of the dump truck during the lifting operation and can widen the threshold range of the critical lift angle to a certain extent and prevent the vehicle from rolling over.

Keywords Dump truck · Active suspension · Lifting operation roll stability · Fuzzy-PID · Simulation

1 Introduction

Dump trucks have problems with lifting operations compared to other heavy commercial vehicles. When the dump truck unloads the cargo under uneven or eccentric load, the body structure is easily deformed and even a rollover accident occurs as the center of gravity increases (Wang et al. (2012); Si et al. (2012)). Therefore, it is necessary to analyze, calculate and test the vehicle roll condition to improve the ability of the dump truck to resist rollover.

The roll model and stability analysis methods of dump trucks are developing in two directions. One is to use the modeling software to establish the rigid-flexible coupled virtual prototype model or directly use the actual prototype to test the vehicle on a special bracket, the second is to use mathematical modeling and calculation methods for research (Baryshnikov (2018)). The former requires the formation of

complex test benches, while the latter requires the creation of complex mathematical models of trucks. Baryshnikov (2018) used mathematical modeling method to derive the dynamic model of the rigid dump truck lifting operation on the longitudinal slope, and studied the lifting stability, and the work in Frimponq et al. (2003) created the robotization and stability control (RASC) model of the mining dump truck, and analyzed the stability of the whole vehicle through simulation. In addition, the stability problems of the dump truck under different lifting conditions by establishing a virtual prototype model were studied in Li et al. (2017a, b), Jiang et al. (2011) and (2012). The virtual prototype model is simple to construct and can visually show the vehicle roll state, but it is difficult to observe and analyze the roll motion laws of various elastic parts of the vehicle such as suspension, tire and cargo box. Because the roll stability of dump truck unloading operation is affected by the elastic deformation of flexible parts (Valladares et al. (2014)), these parts should be considered in establishing the vehicle roll model to ensure high precision.

Furthermore, for the problem of rollover of the dump truck during lifting, currently, real-time monitoring of the lift angle

✉ Mingmao Hu
hu@huat.edu.cn

¹ School of Mechanical Engineering, Hubei University of Automotive Technology, Shiyan 442002, China

of the cargo box is applied to the anti-rollover warning of vehicles. The traditional control method focuses on the intelligent design of electronic, pneumatic and hydraulic control systems, and uses the real-time data collected by sensors fixed on the cargo box and chassis to realize the feedback control of the dynamic lifting system (Hyde et al. (1994), Cham and Tan (2014)). In addition, a single anti-rollover warning is also an indirect control of the lift angle. It is a pre-judgment of the lifting state of the vehicle by comparing the critical lift angle with the actual lift angle measured by the early warning system, and a rollover alarm is issued (Wei et al. (2017) and Valladares (2013)). By limiting the lift angle to near the critical value, the center of gravity offset is prevented from being excessive. Besides, the structural optimization of the lifting mechanism is also applied to the improvement of lifting stability. (see Bai et al. (2012), Li and Wang (2013), Tang et al. (2018) and the references therein). However, the above methods cannot perform active reverse roll control according to the body roll condition to improve the stability of the whole process of vehicle lifting operation.

The control method of the active suspension can effectively improve the roll stability of the vehicle. When the vehicle body rolls to one side, the active suspension on the pressed side can generate the main power opposite to the roll direction and realize the active reverse roll of the vehicle body (Hudha et al. (2014)). To the extent it can alleviate the roll deformation of the suspension. Yu et al. (2008) combined the time to rollover (TTR) warning algorithm with the active suspension control method to improve the roll stability of heavy trucks. Der Westhuizen et al. (2013) used slow active suspension control to suppress the roll of the body and reduce the possibility of rollover. In addition, active or semi-active suspension control is also applied to the improvement in dynamic characteristics in the vertical direction of the vehicle. Attia et al. (2019) designed a linear quadratic regulator (LQR) of the active suspension to improve the road holding stability of the vehicle. Xiao et al. (2020) studied the roll stability control for vehicles with an active roll-resistant electro-hydraulic suspension (RREHS) subsystem. Biglarbegian et al. (2008) proposed a new type of neuro-fuzzy controller to enhance the performance of vehicle semi-active suspension system. Li et al. (2017a, b) and Kong et al. (2015) adopted the fuzzy-PID control of the active and the semi-active suspension to further improve the vibration acceleration of the 2-DOF suspension system. Mustafa et al. (2019) optimized the fuzzy control method based on time delay estimation for the control of active suspension. Lin et al. (2008) proposed a self-organizing fuzzy controller (SOFC), and this control method effectively suppresses vibration of the suspension system. In the above studies, most of the control systems are designed based on simplified linear models, which deviate from the actual operating conditions of dump trucks. Unfortunately, for the improvement in the roll

stability and the dynamic characteristics during the lifting operation of the dump truck, the above control methods have hardly been adopted.

Motivated by the above considerations, this paper studies the anti-rollover early warning control problem of dump trucks lifting based on active suspension. Moreover, compared with exist studies, the main contributions are as follows:

The nonlinear mathematical model of the lift and roll of the dump truck is studied, and the influence of the tire, suspension and cargo box are considered.

In order to actively improve the roll response of each part of the dump truck during the lifting process, the anti-rollover warning control system based on active suspension is designed, and the deviation of the suspension roll deformation is taken as the control variable. The fuzzy-PID control strategy is applied in the control system to make decisions on the control force of the active suspension, and the active adjustment of roll attitude of the dump truck can be realized. In addition, the rollover warning based on rollover evaluation index is combined in the control system.

In this paper, the lift angle, the initial lateral offset of the centroid of the cargo box and the road slope angle are all used as dynamic interference input variables for the control system. Simulation results under the strategies of fuzzy-PID, PID and passive suspension are compared. The results verify that the control method can effectively improve the roll stability of the dump truck during the lifting process and can widen the threshold range of the critical lift angle. Thus, the method in this article can be applied in dump truck lifting operation.

The remainder of this paper is organized as follows: In Sect. 2, the nonlinear mathematical model of the lift and roll of dump truck is established and verified. In Sect. 3, the rollover evaluation index is introduced. Section 4 designs the anti-rollover control system with the fuzzy-PID controller. In Sect. 5, the proposed control strategy is verified through simulation studies under different operating conditions. Section 6 concludes the paper.

2 Modeling and Verification

The vehicle model includes 2 parts: the dynamic model of dump truck roll and lift, these 2 subsystems interact with each other through a hydraulic lift mechanism. The angle and height at which the cargo box is lifted will affect the roll state of the vehicle.

2.1 Dynamic Model of Dump Truck Roll and Lift

The following assumptions and simplifications are given during the model establishment process. First of all, the effect

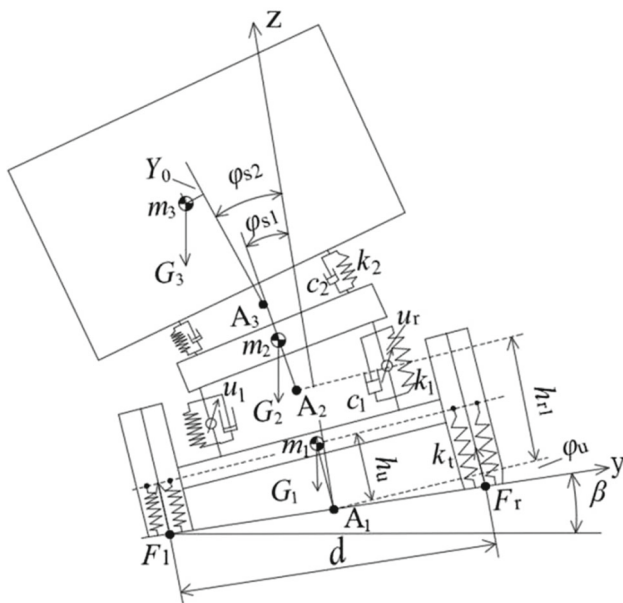


Fig. 1 Dump truck roll model

of the longitudinal movement of the cargo box and the cargo material on the roll of the vehicle is not taken into account during the lifting process, and the cargo does not leave the cargo box during the simulated working condition. Secondly, the sprung mass except the cargo box and the cargo is equivalent to the frame sprung mass, and the part is regarded as a rigid body, and the flexible cargo box is simplified into a mass and a pair of spring dampers, and the distance between the two spring dampers is equal to the distance between the flip hinges. Thirdly, the lateral deformation of the tire, and all tires do not slip laterally on the road surface are ignored. The roll model of the dump truck during the lifting of the cargo box is shown in Fig. 1.

Where m_1 is the unsprung mass of the vehicle; m_2 is the sprung mass of the frame; m_3 is the mass of the cargo box and cargo; A_1 , A_2 and A_3 are the roll centers of m_1 , m_2 and m_3 ; φ_u , φ_{s1} and φ_{s2} are the roll angles of m_1 , m_2 and m_3 ; G_1 , G_2 and G_3 are the gravity of each part of the vehicle; β is the lateral slope angle of pavement; Y_0 is the initial lateral offset of the centroid of m_3 ; d is the wheelbase; h_u is the roll length of m_1 ; h_{r1} is the initial height of the roll center A_2 ; u_l and u_r are the active suspensions control forces; F_l and F_r are vertical loads acting on the left and right wheels; k_t is the vertical stiffness of a single tire; k_1 and k_2 are the stiffness of the suspension spring and the equivalent stiffness of the box when lifting; c_1 and c_2 are the equivalent damping coefficients of the suspension and cargo.

The target dump truck is set to the front cylinder straight push lift mode, the lower end of the cylinder is connected to the frame through the spherical sub-hinge, and the upper end is connected to the cargo box through the rotary sub-hinge.

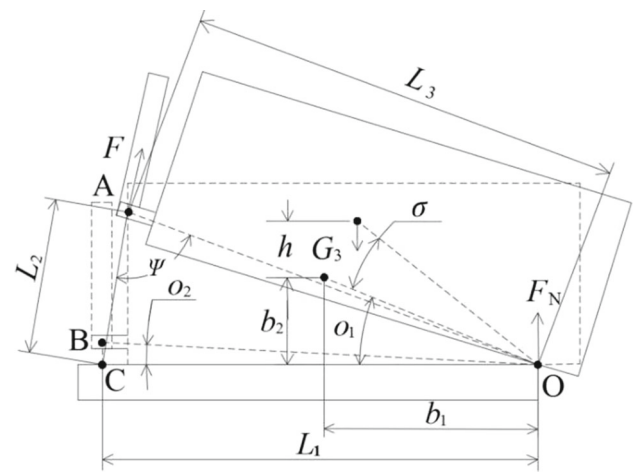


Fig. 2 Dump truck lift model

The vehicle lift model when the road surface is a horizontal plane and the vehicle does not roll is shown in Fig. 2. During the lifting process, the cargo box is subjected to gravity G_3 , the cylinder lifting force F and the supporting force F_N at the hinge point of the container frame.

Where L_1 is the distance between point C and point O; L_2 is the distance between point C and point A; L_3 is the distance from point A to point O; b_1 and b_2 are the vertical distance and horizontal distance between the centroid of the cargo box to the line segment OC and point O; o_1 is the angle between the line segment OC and the centroid of the cargo box to the point O when the cargo box is not lifted; o_2 is also the angle between the line segment OC and the line segment OB when the cargo box is not lifted; ψ is the angle between the line segment AC and the line segment AO; h is the height that the centroid of the cargo box rise vertically relative to the horizontal road surface; σ is the lifting angle. The expression relationships of o_1 , o_2 , L_2 , ψ and h are obtained from the geometric relationships:

$$\begin{cases} o_1 = \arctan(b_2/b_1) \\ o_2 = \arccos(L_1/L_3) \\ L_2 = \sqrt{L_1^2 + L_3^2 - 2L_1L_3 \cos(o_2 + \sigma)} \\ \cos \psi = (L_2^2 + L_3^2 - L_1^2) / 2L_2L_3 \\ h = 2\sqrt{b_1^2 + b_2^2} \sin(\sigma/2) \cos(\sigma/2 + o_1) \end{cases} \quad (1)$$

When the road surface has a lateral slope angle, the vehicle will tilt as a whole and roll. During the lifting process of the cargo box, since the torsional torque of the entire cargo box is mainly borne by the bottom plate of the cargo box, the torsional resistance is poor, and when the center of gravity of the cargo box is shifted, it is easily twisted and deformed.

(Tian et al. (2010)). So the vertical distance of the centroid of m_3 from the slope can be expressed as $h \cos \varphi_{s2}$.

The vehicle dynamics equation is derived with the Lagrange analysis mechanics method. Based on this method, a 4-DOF nonlinear dynamic model including vehicle lift and roll motion is established.

Cargo box turnover equation is given as

$$\begin{aligned} P_1 \ddot{\sigma} + P_2 \ddot{\varphi}_u \cos(\sigma + \sigma_1) \sin(\varphi_{s2} - \varphi_u) + P_3 \ddot{\varphi}_{s1} \cos(\sigma + \sigma_1) \sin(\varphi_{s2} - \varphi_{s1}) + P_4 Y_0 \ddot{\varphi}_{s2} \cos(\sigma + \sigma_1) \\ = P_2 \dot{\varphi}_u^2 \cos(\sigma + \sigma_1) \cos(\varphi_{s2} - \varphi_u) + P_3 \dot{\varphi}_{s1}^2 \cos(\sigma + \sigma_1) \cos(\varphi_{s2} - \varphi_{s1}) + P_5 \dot{\varphi}_{s2}^2 \cos(\sigma + \sigma_1) \\ - P_6 \cos(\sigma + \sigma_1) \cos(\varphi_{s2} + \beta) + F L_3 \sin \psi. \end{aligned} \quad (2)$$

Unsprung mass roll motion equation is given as

$$\begin{aligned} P_2 \ddot{\sigma} \cos(\sigma + \sigma_1) \sin(\varphi_{s2} - \varphi_u) + P_7 \ddot{\varphi}_u + P_8 \ddot{\varphi}_{s1} \cos(\varphi_{s1} - \varphi_u) + (P_9 \cos(\varphi_{s2} - \varphi_u) + P_{10} Y_0 \sin(\varphi_u - \varphi_{s2})) \ddot{\varphi}_{s2} \\ = -2 P_2 \dot{\sigma} \dot{\varphi}_{s2} \cos(\sigma + \sigma_1) \cos(\varphi_{s2} - \varphi_u) + P_{11} \dot{\sigma}^2 \sin(\sigma + \sigma_1) + P_8 \dot{\varphi}_{s1}^2 \sin(\varphi_{s1} - \varphi_u) \\ + \dot{\varphi}_{s2}^2 (P_9 \sin(\varphi_{s2} - \varphi_u) + P_{10} Y_0 \cos(\varphi_u - \varphi_{s2})) + P_{12} \sin(\varphi_u + \beta) - P_{13} \tan \varphi_u (1 + \tan^2 \varphi_u) \\ + P_{14} \tan(\varphi_{s1} - \varphi_u) (1 + \tan^2(\varphi_{s1} - \varphi_u)) + P_{15} (\dot{\varphi}_{s1} - \dot{\varphi}_u) (1 + \tan^2(\varphi_{s1} - \varphi_u))^2 + (u_l + u_r) d_1 / 2. \end{aligned} \quad (3)$$

Frame sprung mass roll motion equation is given as

$$\begin{aligned} P_3 \ddot{\sigma} \cos(\sigma + \sigma_1) \sin(\varphi_{s2} - \varphi_{s1}) + P_8 \ddot{\varphi}_u \cos(\varphi_u - \varphi_{s1}) + P_{16} \ddot{\varphi}_{s1} + (P_{17} \cos(\varphi_{s2} - \varphi_{s1}) + P_{18} Y_0 \sin(\varphi_{s1} - \varphi_{s2})) \ddot{\varphi}_{s2} \\ = -2 P_3 \dot{\sigma} \dot{\varphi}_{s2} \cos(\sigma + \sigma_1) \cos(\varphi_{s2} - \varphi_{s1}) + P_{11} \dot{\sigma}^2 \sin(\sigma + \sigma_1) + P_8 \dot{\varphi}_u^2 \sin(\varphi_u - \varphi_{s1}) + (P_{17} \sin(\varphi_{s2} - \varphi_{s1}) + P_{18} Y_0 \cos(\varphi_{s1} - \varphi_{s2})) \dot{\varphi}_{s2}^2 \\ + P_{19} \sin(\varphi_{s1} + \beta) - P_{14} \tan(\varphi_{s1} - \varphi_u) (1 + \tan^2(\varphi_{s1} - \varphi_u)) + P_{20} \tan(\varphi_{s2} - \varphi_{s1}) (1 + \tan^2(\varphi_{s2} - \varphi_{s1})) + P_{15} (\dot{\varphi}_u - \dot{\varphi}_{s1}) (1 + \tan^2(\varphi_{s1} - \varphi_u))^2 \\ + P_{21} (\dot{\varphi}_{s2} - \dot{\varphi}_{s1}) (1 + \tan^2(\varphi_{s2} - \varphi_{s1}))^2 - F (h_{r2} - h_{r1}) \sin(\psi + \sigma_2 + \sigma) \sin(\varphi_{s2} - \varphi_{s1}) - (u_l + u_r) d_1 / 2. \end{aligned} \quad (4)$$

And the cargo roll motion equation is given as

$$\begin{aligned} P_4 Y_0 \ddot{\sigma} \cos(\sigma + \sigma_1) + (P_9 \cos(\varphi_u - \varphi_{s2}) + P_{10} Y_0 \sin(\varphi_u - \varphi_{s2})) \ddot{\varphi}_u + (P_{17} \cos(\varphi_{s1} - \varphi_{s2}) + P_{18} Y_0 \sin(\varphi_{s1} - \varphi_{s2})) \ddot{\varphi}_{s1} + P_{22} \ddot{\varphi}_{s2} \\ = -2 P_5 \dot{\sigma} \dot{\varphi}_{s2} \cos(\sigma + \sigma_1) - P_{11} \dot{\sigma}^2 \sin(\sigma + \sigma_1) - (P_9 \sin(\varphi_{s2} - \varphi_u) + P_{10} Y_0 \cos(\varphi_u - \varphi_{s2})) \dot{\varphi}_u^2 \\ - (P_{17} \sin(\varphi_{s2} - \varphi_{s1}) + P_{18} Y_0 \cos(\varphi_{s1} - \varphi_{s2})) \dot{\varphi}_{s1}^2 + P_{23} \sin(\varphi_{s2} + \beta) + P_{24} Y_0 \cos(\varphi_{s2} + \beta) \\ - P_{20} \tan(\varphi_{s2} - \varphi_{s1}) (1 + \tan^2(\varphi_{s2} - \varphi_{s1})) + P_{21} (\dot{\varphi}_{s1} - \dot{\varphi}_{s2}) (1 + \tan^2(\varphi_{s2} - \varphi_{s1}))^2. \end{aligned} \quad (5)$$

From Eqs. (2–5): $P_1 = m_3(b_1^2 + b_2^2) + I_4$; $P_2 = m_3 h_{r1} \sqrt{b_1^2 + b_2^2}$; $P_3 = m_3(h_{r2} - h_{r1}) \sqrt{b_1^2 + b_2^2}$; $P_4 = -m_3 \sqrt{b_1^2 + b_2^2}$; $P_5 = m_3(h + h_3 - h_{r2}) \sqrt{b_1^2 + b_2^2}$; $P_6 = m_3 g \sqrt{b_1^2 + b_2^2}$; $P_7 = m_1 h_u^2 + m_2 h_{r1}^2 + m_3 h_{r1}^2 + I_1$; $P_8 = m_2 h_{r1}(h_2 - h_{r1}) + m_3 h_{r1}(h_{r2} - h_{r1})$; $P_9 = m_3 h_{r1}(h + h_3 - h_{r2})$; $P_{10} = m_3 h_{r1}$; $P_{11} = m_3 \sqrt{b_1^2 + b_2^2}$; $P_{12} = (m_1 h_u + m_2 h_{r1} + m_3 h_{r1})g$; $P_{13} = k_t d^2$; $P_{14} = k_1 d_1^2 / 2$; $P_{15} = c_1 d_1^2 / 2$; $P_{16} = m_2(h_2 - h_{r1})^2 + m_3(h_{r2} - h_{r1})^2 + I_2$; $P_{17} = m_3(h_{r2} - h_{r1})(h + h_3 - h_{r2})$; $P_{18} = m_3(h_{r2} - h_{r1})$; $P_{19} = m_2 g(h_2 - h_{r1}) + m_3 g(h_{r2} - h_{r1})$; $P_{20} =$

$k_2 d_2^2 / 2$; $P_{21} = c_2 d_2^2 / 2$; $P_{22} = m_3((h + h_3 - h_{r2})^2 + Y_0^2) + I_3$; $P_{23} = m_3 g(h + h_3 - h_{r2})$; $P_{24} = m_3 g$, where I_1 , I_2 , and I_3 are moments of inertia of the roll of each part of the vehicle; I_4 is the moment of inertia of the cargo box turnover;

h_2 and h_3 are the initial centroid heights of the frame sprung mass and the cargo box; h_{r2} is the initial height of the roll center A_3 ; d_1 and d_2 are the left and right side suspension spacing and the container flip hinge spacing.

The unsprung mass roll angle φ_u , the frame sprung mass roll angle φ_{s1} and the cargo box roll angle φ_{s2} are selected as the output variables of the model. The lifting angle σ , the initial lateral offset Y_0 and the lateral slope angle of pavement β are used as input variables of the model. In order to simulate the rolling process of the vehicle from loading to driving into the slope and then lifting, and also avoid the large fluctuations in the system, the disturbance inputs processes are uniform,

so there is $\ddot{\sigma} = 0$. The vehicle nonlinear roll matrix motion equation can be obtained from Eqs. (3–5) as

$$\mathbf{M}(\mathbf{q})\ddot{\mathbf{q}} + \mathbf{C}(\mathbf{q}, \dot{\mathbf{q}})\dot{\mathbf{q}} + \mathbf{G}(\mathbf{q}) = \mathbf{f}_Q \quad (6)$$

Where $\mathbf{q} = [\varphi_u \ \varphi_{s1} \ \varphi_{s2}]^T$, $\mathbf{M}(\mathbf{q}) =$

$$\begin{bmatrix} P_7 & P_8 \cos(\varphi_{s1} - \varphi_u) & P_9 \cos(\varphi_{s2} - \varphi_u) \\ P_8 \cos(\varphi_{s1} - \varphi_u) & P_{16} & P_{17} \cos(\varphi_{s2} - \varphi_{s1}) \\ P_9 \cos(\varphi_{s2} - \varphi_u) & P_{17} \cos(\varphi_{s2} - \varphi_{s1}) & P_{22} \end{bmatrix}, \mathbf{C}$$

$$(\mathbf{q}, \dot{\mathbf{q}}) = \begin{bmatrix} P_{15}(1 + \tan^2(\varphi_{s1} - \varphi_u))^2 & -P_8\dot{\varphi}_{s1} \sin(\varphi_{s1} - \varphi_u) & -\dot{\varphi}_{s2}(P_9 \sin(\varphi_{s2} - \varphi_u) + P_{10}Y_0 \cos(\varphi_u - \varphi_{s2})) \\ -P_8\dot{\varphi}_u \sin(\varphi_u - \varphi_{s1}) & P_{15}(1 + \tan^2(\varphi_{s1} - \varphi_u))^2 & -\dot{\varphi}_{s2}(P_{17} \sin(\varphi_{s2} - \varphi_{s1}) + P_{18}Y_0 \cos(\varphi_{s1} - \varphi_{s2})) \\ -P_{15}(1 + \tan^2(\varphi_{s1} - \varphi_u))^2 & +P_{21}(1 + \tan^2(\varphi_{s2} - \varphi_{s1}))^2 & -P_{21}(1 + \tan^2(\varphi_{s2} - \varphi_{s1}))^2 \\ \dot{\varphi}_u(P_9 \sin(\varphi_{s2} - \varphi_u) + P_{10}Y_0 \cos(\varphi_u - \varphi_{s2})) & \dot{\varphi}_{s1}(P_{17} \sin(\varphi_{s2} - \varphi_{s1}) + P_{18}Y_0 \cos(\varphi_{s1} - \varphi_{s2})) & P_{21}(1 + \tan^2(\varphi_{s2} - \varphi_{s1}))^2 \\ & -P_{21}(1 + \tan^2(\varphi_{s2} - \varphi_{s1}))^2 & \end{bmatrix}, \mathbf{G}$$

$$(\mathbf{q}) = \begin{bmatrix} -P_{12} \sin(\varphi_u + \beta) + P_{13} \tan \varphi_u (1 + \tan^2 \varphi_u) \\ -P_{14} \tan(\varphi_{s1} - \varphi_u) (1 + \tan^2(\varphi_{s1} - \varphi_u)) \\ -P_{19} \sin(\varphi_{s1} + \beta) + P_{14} \tan(\varphi_{s1} - \varphi_u) (1 + \tan^2(\varphi_{s1} - \varphi_u)) \\ -P_{20} \tan(\varphi_{s2} - \varphi_{s1}) (1 + \tan^2(\varphi_{s2} - \varphi_{s1})) \\ -P_{23} \sin(\varphi_{s2} + \beta) - P_{24}Y_0 \cos(\varphi_{s2} + \beta) \\ +P_{20} \tan(\varphi_{s2} - \varphi_{s1}) (1 + \tan^2(\varphi_{s2} - \varphi_{s1})) \end{bmatrix}, \mathbf{f}_Q =$$

$$\begin{bmatrix} (u_l + u_r)d_1/2 \\ -F(h_{r2} - h_{r1}) \sin(\psi + o_2 + \sigma) \sin(\varphi_{s2} - \varphi_{s1}) - (u_l + u_r)d_1/2 \\ 0 \end{bmatrix},$$

where \mathbf{M} is a symmetric positive definite inertia matrix; \mathbf{C} is a matrix containing Coriolis forces, centrifugal forces and damping generalized forces caused by the damping of suspension and cargo box; \mathbf{G} is a matrix containing derived terms from potential energy, such as gravity and elastic generalized forces caused by the elastic deformation of the tire, suspension, and torsional deformation of the cargo box; \mathbf{f}_Q is an input generalized force vector, and the lifting force F is related to the lifting angle (see the cylinder thrust analysis in Sect. 2 (Theoretical mechanics analysis of dump truck lifting operation) of the work in Yao (2016)), which is obtained by Eq. (2) when the lifting angle σ is known.

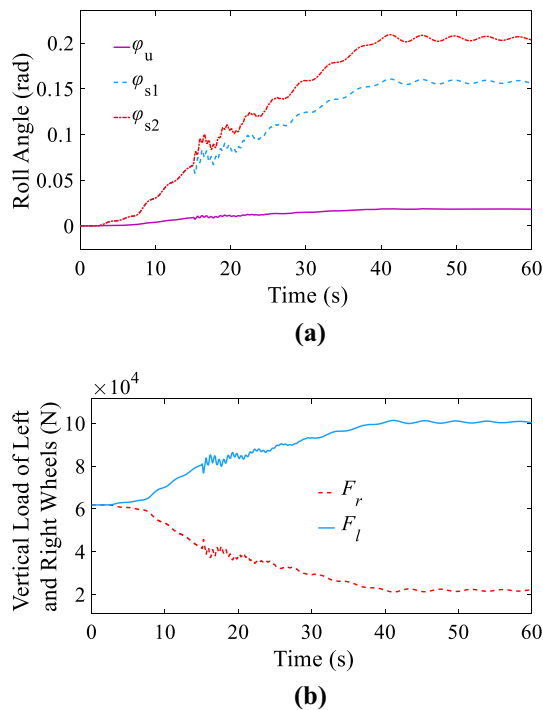
2.2 Model Dynamics Verification

The dynamic characteristics of the model are verified in the MATLAB/Simulink simulation environment. Slowly input initial lateral offset to 0.05 m within 2–7 s during the simulation. Then the lateral slope angle of pavement is input to 8° at a speed of $1^\circ/\text{s}$, and finally the lifting angle is input at a speed of $2^\circ/\text{s}$, the maximum lift angle is 50° . The main relevant parameters of a dump truck are shown in Table 1.

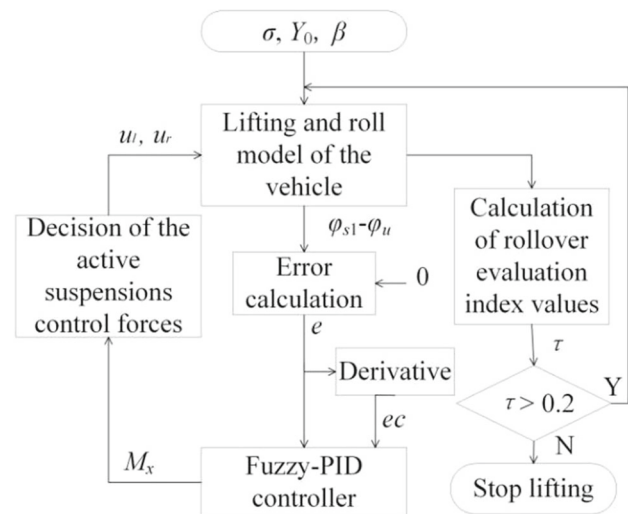
Simulation is carried out in the case of a passive suspension ($u_l = u_r = 0$). The roll angles of each part of the vehicle and the vertical load of the left and right tires are obtained, as shown in Fig. 3.

Table 1 Main relevant parameters of the dump truck

Parameters	Values	Units
m_1	1.200	kg
m_2	5.420	kg
m_3	6.000	kg
h_u	0.52	m
h_2	1.12	m
h_3	2	m
I_1	3.390	kg·m ²
I_2	15.200	kg·m ²
I_3	18.260	kg·m ²
h_{r1}	0.62	m
h_{r2}	1.30	m
d	1.86	m
d_1	1.15	m
d_2	0.9	m
k_1	650.000	N/m
k_2	2.182.000	N/m
k_t	1.150.000	N/m
c_1	20.000	N·s·m ⁻¹
c_2	1.000	N·s·m ⁻¹

**Fig. 3** Dynamic simulation results. **a** Roll angle results curves, **b** Vertical load curves of left and right wheels

Before inputting initial lateral offset and the lateral slope angle of pavement, the roll angle of each part of the vehicle is zero, and the load of the left and right tires is equal ($F_l = F_r$).

**Fig. 4** Active anti-rollover warning control structure

With the input of initial lateral offset and the lateral slope angle of pavement before lifting, the unsprung mass roll angle ϕ_u and the sprung mass roll angles (ϕ_{s1} and ϕ_{s2} , at this stage, $\phi_{s1} = \phi_{s2}$) increase slowly, and the right tire load gradually shifts to the left side. The vehicle begin to lift when it is simulated for 15 s. As the lifting operation progresses, the roll angle of each part is further increased to a different extent, and the vehicle load continued to shift to the left side. After 40 s, the cargo box stops lifting ($\sigma = 50^\circ$), and the roll angles of the parts and the vertical load of the tires fluctuate slightly around the corresponding values and tend to be stable within a reasonable range. So the variables of the vehicle model respond well to the input, indicating that the model can accurately reflect the dynamic characteristics of the vehicle.

3 Rollover Evaluation Index

According to the provisions of GB7258-2017 ‘Technical specifications for safety of power-driven vehicles operating on roads’ (Chinese standard), the load on the steering shaft of the dump truck should not be less than 20% of the total weight of the dump truck regardless of the no-load or full load. If the ratio of the non-bearing wheel vertical load to the total vehicle weight is less than 0.2, the vehicle has a risk of rollover, so the rollover critical lift angle is given when the value of ratio is 0.2.

The expressions of the vertical loads F_l and F_r of the left and right tires during the lifting operation on the lateral slope are

$$\begin{cases} F_l = 2k_t(z_{t0} + (d \tan \varphi_u)/2) \\ F_r = 2k_t(z_{t0} - (d \tan \varphi_u)/2) \end{cases} \quad (7)$$

where z_{t0} is the initial deformation amount of the tire before the vehicle roll, and it is calculated by the following formula:

$$z_{t0} = \cos \beta (G_1 + G_2 + G_3) / 4k_t \quad (8)$$

The ratio of the vertical load of the non-bearing wheel on the right side to the total weight of the vehicle is

$$\tau = F_r / (G_1 + G_2 + G_3) \quad (9)$$

where the ratio τ is a evaluation index for the dump truck rollover. In this paper, if there is no rollover accident occurs during the vehicle lifting operation, it should satisfy

$$0.2 \leq \tau \leq 0.5 \quad (10)$$

if τ is closer to 0.5, it indicates that the stability of the vehicle is better, and vice versa. If $\tau = 0$, it indicates that the vehicle has rolled over. $\tau = 0.2$ is considered as the threshold for the rollover warning.

4 Anti-Rollover Control System Design

In this paper, the anti-rollover control is based on the control method of the active suspension. The active forces (u_l and u_r) of the left and right suspensions are properly distributed to achieve the reverse roll of the vehicle, and the forces also suppress the left and right sway of the vehicle. The fuzzy-PID control strategy is used to control the active suspension and obtain the required reverse roll moment M_x . In the control system, the lifting angle σ , the initial lateral offset Y_0 and the lateral slope angle of pavement β are the interference input, the suspension roll deformation amount ($\varphi_{s1} - \varphi_u = 0$) is the reference input of the ideal target, and the error ($e = \varphi_u - \varphi_{s1}$) is a control variable. In addition, the evaluation indicator τ will be used to conduct rollover warning. The evaluation indicator is calculated and detected in real time, and if it is no more than 0.2, the vehicle will stop lifting, and the active anti-rollover warning control structure is shown in Fig. 4.

The fuzzy controller adopts a two-input and three-output configuration, and the system deviation e and the deviation change rate ec are inputs, the adjustments of the PID parameters (Δk_p , Δk_i and Δk_d) are outputs. The three parameters of the PID controller are adjusted in real time using fuzzy rules. The adjusted PID parameter is expressed as

$$\begin{cases} k_p = k_{p0} + \Delta k_p \\ k_i = k_{i0} + \Delta k_i \\ k_d = k_{d0} + \Delta k_d \end{cases} \quad (11)$$

where k_{p0} , k_{i0} and k_{d0} are the initial tuning parameters of the PID controller. In this paper, through multiple simulation

experiments, the values of k_{p0} , k_{i0} and k_{d0} are, respectively, determined to be 25, 6 and 12. Then the required reverse roll moment decision is

$$M_x(t) = k_p e(t) + k_i \int_0^t e(t) dt + k_d \frac{de(t)}{dt} \quad (12)$$

The input and output linguistic variables of the fuzzy controller are {NB, NM, NS, ZE, PS, PM, PB}, that are {negative big, negative medium, negative small, zero, positive small, positive medium, positive big}. According to the simulation test, the basic domains of the input and output signals are selected as $e \in [-0.07, 0.07]$, $ec \in [-0.1, 0.1]$, $\Delta k_p \in [-60, 60]$, $\Delta k_i \in [-9, 9]$, $\Delta k_d \in [-10, 10]$. The quantization factors of the input and output signals are $k_e = 43$, $k_{ec} = 30$, $k_{up} = 20$, $k_{ui} = 3$, $k_{ud} = 10/3$, and the inputs and outputs are subject to the distribution of the trigonometric membership function.

In addition, it is necessary to design precise fuzzy control rules to get better control effects. However, control rules are generally designed based on the designer's experience and relevant materials. The design principles are referred to Khan and Rapal (2006). Firstly, if $|e|$ is large, a large k_p and a small k_d are taken, so the system response speed will be faster and has better target tracking performance. Secondly, if $|e|$ is a medium size, a small k_p and an appropriate size k_i and k_d are taken to reduce the overshoot of the system response. Finally, if $|e|$ is small, a large k_p , k_i and an appropriate size of k_d are taken to avoid oscillation of the system near the set value, so the system will have a better steady state performance, and the fuzzy control rules are shown in Table 2.

The reverse roll moment M_x obtained from Eq. (12) is used to make a decision on the active suspension control forces u_l and u_r , and they take the moment between the roll center A_2 to obtain the relationship between M_x and u_l , u_r :

$$M_x = (u_l + u_r) d_1 / 2 = u_l d_1 = u_r d_1 \quad (13)$$

where u_l and u_r are equal in size and opposite in direction. Therefore, the decision expression of the active control force is given as:

$$u_l = u_r = M_x / d_1 \quad (14)$$

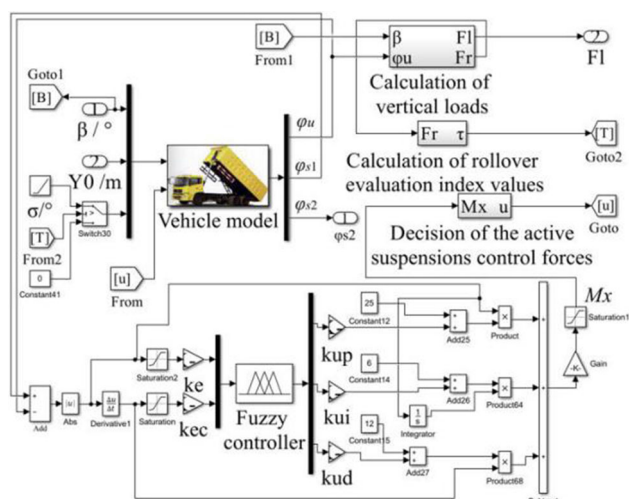
Finally, the anti-rollover control system simulation model is shown in Fig. 5.

5 Results and Discussion

The fuzzy-PID control and PID control strategy of the active suspension are used to numerically analyze the rollover

Table 2 Δk_p , Δk_i and Δk_d fuzzy control rules

U		ec						
		NB	NM	NS	ZE	PS	PM	PB
e	NB	PB/NB/PS	PB/NB/NS	PB/NM/NB	PM/NM/NB	PB/NS/NB	PS/ZE/NM	ZE/ZE/PS
	NM	PB/NB/PS	PB/NB/NS	PB/NM/NB	PM/NS/NM	PS/NS/NM	ZE/ZE/NS	NS/ZE/ZE
	NS	PB/NB/ZE	PM/NM/NS	PM/NS/NM	PS/NS/NM	ZE/ZE/NS	NS/PS/NS	NM/PS/ZE
	ZE	PM/NM/ZE	PM/NM/NS	PS/NS/NS	ZE/ZE/NS	NS/PS/NS	NM/PM/NS	NM/PM/ZE
	PS	PM/NM/ZE	PS/NS/ZE	ZE/ZE/ZE	NS/PS/ZE	NM/PS/NS	PM/NM/ZE	NM/PB/ZE
	PM	PS/ZE/PB	ZE/ZE/PS	NS/PS/PS	NM/PS/ PS	NM/PM/PS	NB/PB/PS	NB/PB/PB
	PB	ZE/ZE/PB	NS/ZE/PM	NM/PS/ PM	NM/PM/PM	NB/PM/PS	NB/PB/PS	NB/PB/PB

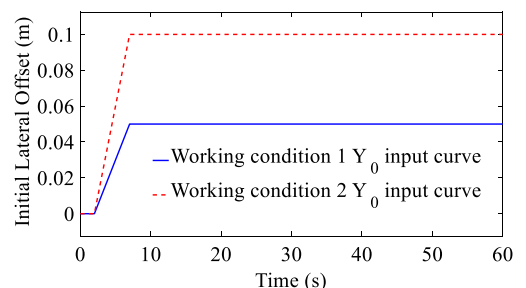
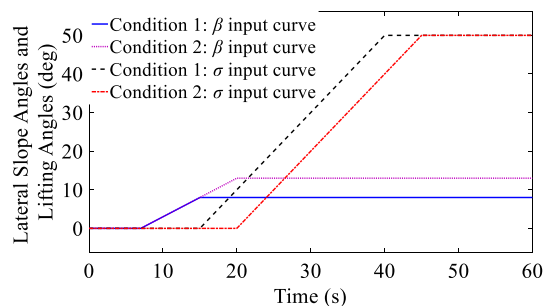
**Fig. 5** Control system simulation model

resistance of the dump truck, which are compared with the stability of the traditional passive suspension vehicle. Then, the numerical calculation analysis of the critical lift angle under different working conditions are carried out.

Two simulation conditions are set. In working condition 1, the lateral slope angle of pavement is 8° , the initial lateral offset is 0.05 m, and the lifting angle is 50° . In working condition 2, the lateral slope angle of pavement is 13° , the initial lateral offset is 0.1 m and the maximum lifting angle is 50° . The simulation was performed in the MATLAB/Simulink environment, and the input curves of the control system are shown in Fig. 6.

5.1 Comparison of Rollover Evaluation Index Values

Figure 7 shows the simulation results of the rollover evaluation index values under the active suspension and the passive suspension. It can be seen from the figure that the two control strategies of the active suspension can effectively improve the roll stability of the vehicle. However, as the rigidity of

**(a)****(b)****Fig. 6** Input curves of the control system. **a** Y_0 input curves, and **b** β and σ input curves

the cargo box decreases and the height of the center of mass increases at the beginning of lifting, the system will oscillate. We can also see that in the initial stage of the lift, the curve oscillations under the fuzzy-PID and PID control strategies are roughly the same. Because in the early stage of lifting, the control variable e is relatively small, which leads to insufficient output of the controller to the control force. In further research, the problem of insufficient control power could be solved by adaptively adjusting the size of the quantization factor of the input and output signals.

In addition, compared with the PID control, the fuzzy-PID control increases the minimum value of the rollover evaluation index, and less time needed to stabilize the vehicle after the lifting operation and the danger of vehicle rollover is

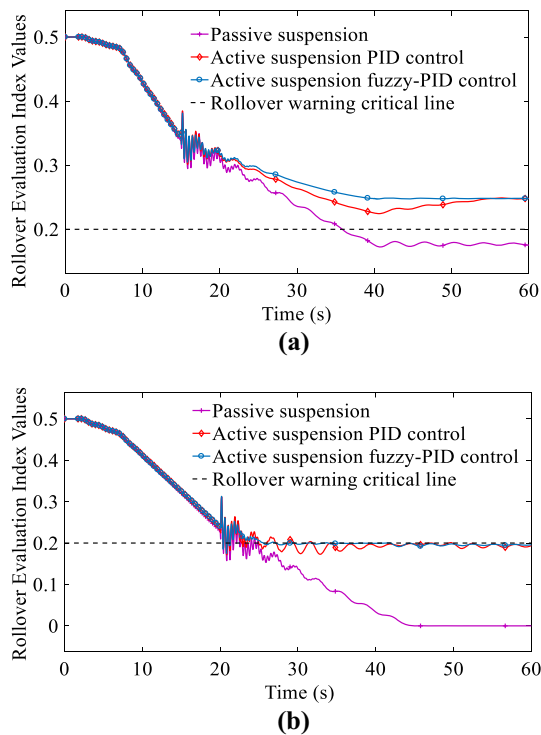


Fig. 7 Rollover evaluation index curves. **a** Rollover evaluation index values in case of working condition 1, and **b** Rollover evaluation index values in case of working condition 2

avoided. In working condition 1, the index value of the traditional passive suspension vehicle has crossed the rollover warning critical line before the end of the lift. In working condition 2, the index value of the passive suspension vehicle crossed the rollover warning critical line in a short time after lifting, and finally reached zero, and this means the vehicle has rolled over. But the index values are all stable around 0.2 after the warning control, indicating that the control system has a better early warning effect.

5.2 Analysis of the Roll Angle of Each Part of the Vehicle

Figure 8 shows the whole process variation curve of the unsprung mass roll angle, the frame sprung mass roll angle and the cargo box roll angle under the working condition 1. At the beginning of the lift, the body vibration amplitude is large, but in the subsequent lifting process, the roll angle of each part of the vehicle under controlled is reduced. In addition, the body vibration amplitude and the number of times is significantly reduced. When the lift is over, the reverse roll moment under PID control continues to increase, and the roll angle of each part is significantly reduced. Although there is no obvious shock, the stability time of vehicle is prolonged. Compared with the fuzzy-PID control, the control effect is slightly worse.

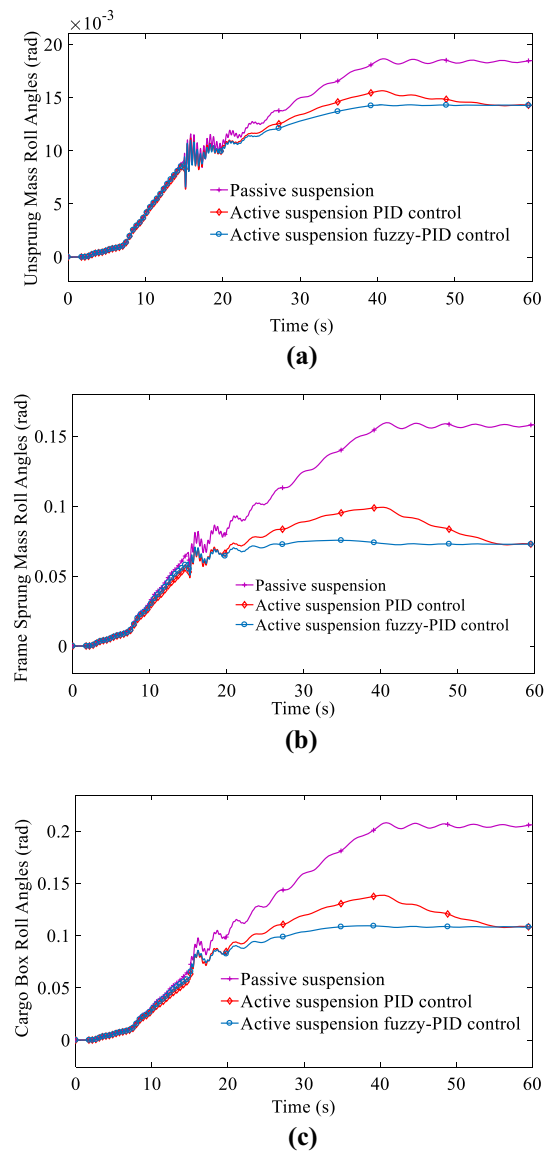


Fig. 8 Roll curve of each part of the vehicle. **a** Unsprung mass roll angle, **b** Frame sprung mass roll angle, and **c** Cargo box roll angle

5.3 Numerical Analysis of Critical Lift Angle

Table 3 gives the comparison results of the critical lift angle and the improvement effect under different lifting conditions. It can be seen from the table that the critical lift angle of the vehicle gradually decreases with the increase in the initial lateral offset and the lateral slope angle of pavement. In most working conditions, compared with the traditional passive suspension, the critical lift angle after the active suspension anti-rollover warning control is increased to some extent, but the effect of the fuzzy-PID control strategy on the critical lift angle is improved. However, the value of the rollover evaluation index is close to the critical line before the cargo box is lifted in some extreme conditions, and the body oscillate

Table 3 Comparison of critical lift angle(deg) and improvement effect under different conditions

Initial lateral offset Y_0 (m)	Lateral slope angle of pavement β (deg)	Passive suspension	Active suspension fuzzy-PID control		Active suspension PID control	
0	9.0	40.0	—		—	
	10	32.0	—		42.0	31.25%
	11	25.4	37.0	45.67%	32.0	25.98%
	12	19.0	27.0	42.11%	24.6	29.47%
	13	13.0	19.6	50.77%	18.2	40.00%
	14	7.00	13.4	91.43%	12.6	80.00%
	8.0	42.0	—		—	
0.05	9.0	33.3	—		47.6	42.94%
	10	26.0	42.0	61.54%	34.0	30.77%
	11	19.2	29.4	53.13%	25.6	33.33%
	12	13.0	21.0	61.54%	18.8	44.62%
	13	7.00	14.2	102.9%	12.8	82.86%
	8.0	34.0	—		—	
	9.0	26.4	43.6	65.15%	38.0	43.94%
0.10	10	20.0	33.0	65.00%	26.6	33.00%
	11	13.2	23.2	75.76%	19.0	43.94%
	12	7.00	15.8	125.7%	12.8	82.86%

amplitude at the beginning of the lift is large, so that the index value quickly crosses the critical line. In this case, the critical lift angles with and without control are small. In general, the control system can widen the threshold range of the critical lift angle to a certain extent, and improve the adaptability of the dump truck unloading operation.

6 Conclusions

This paper studies the anti-rollover early warning control problem of dump trucks lifting based on active suspension. The highly accurate nonlinear model of the dump truck lifting operation was established by considering the influence of elastic deformation of the tire, suspension, and torsional deformation of the cargo box, and the applicability of the model was verified from the perspective of dynamic characteristics. Moreover, the anti-rollover fuzzy-PID warning control system based on active suspension was designed. The improvement effect of the control system is analyzed from the aspects of rollover evaluation index, roll angle and critical lifting angle. Finally, simulation results are provided to verify the proposed method could widen the threshold range of the critical lift angle, improve the adaptability of the dump truck to the road environment, and effectively prevent the vehicle from rolling over.

Acknowledgements This paper is supported by the Hubei Intelligent Manufacturing and Intelligent Travel Engineering Technology Research Center Innovation Platform Construction Fund (Grant No.

2019ZYYD014); Hubei Key Laboratory of Automotive Power Transmission and Electronic Control (Hubei University of Automotive Technology) Fund (Grant No. ZDK1201802).

References

- Attia, T., Vamvoudakis, K. G., Kochersberger, K., Bird, J., & Furukawa, T. (2019). Simultaneous dynamic system estimation and optimal control of vehicle active suspension. *Vehicle System Dynamics*, 57(10), 1467–1493. <https://doi.org/10.1080/00423114.2018.1521000>
- Bai, H. Y., Fu, C. Y., & Zhang, X. Z. (2012). Kinematics analysis of heavy dump truck lifting mechanism. *Advanced Materials Research*, 472–475, 2245–2250. <https://doi.org/10.4028/www.scientific.net/amr.472-475.2245>
- Baryshnikov, Y. N. (2018). Computing experiment for unloading dumper truck at a sloping pad. *IOP Conference Series: Materials Science and Engineering*. <https://doi.org/10.1088/1757-899X/468/1/012022>
- Biglarbegian, M., Melek, W., & Golnaraghi, F. (2008). A novel neuro-fuzzy controller to enhance the performance of vehicle semi-active suspension systems. *Vehicle System Dynamics*, 46(8), 691–711. <https://doi.org/10.1080/00423110701585420>
- Cham, C. L., & Tan, W. H. (2014). Design of an intelligent electronic system for dump truck tip-over prevention. *Informacije Midem Journal of Microelectronics Electronic Components and Materials*, 44(2), 152–158.
- Der Westhuizen, S. F., & Els, P. S. (2013). Slow active suspension control for rollover prevention. *Journal of Terramechanics*, 50(1), 29–36. <https://doi.org/10.1016/j.jterra.2012.10.001>
- Frimponq, S., Chanqirwa, R., & Szymanski, J. (2003). Simulation of automated dump trucks for large scale surface mining operations. *International Journal of Mining, Reclamation and Environment*, 17(3), 183–195. <https://doi.org/10.1076/ijsm.17.3.183.14770>

- Hudha, K., Kadir, Z. A., & Jamaluddin, H. (2014). Simulation and experimental evaluations on the performance of pneumatically actuated active roll control suspension system for improving vehicle lateral dynamics performance. *International Journal of Vehicle Design*, 64(1), 72–100. <https://doi.org/10.1504/IJVD.2014.057771>
- Hyde, T. H., Fessler, H., & Pickering, S. G. (1994). A method for assessing the rollover stability of articulated tipping trailer units under tipping conditions. *Proceedings of the Institution of Mechanical Engineers, Part D: Journal of Automobile Engineering*, 208(3), 161–173. https://doi.org/10.1243/PIME_PROC_1994_208_179_02
- Jiang, R. C., Liu, D. W., Chen, H. M., & Gao, Z. G. (2011). Roll characteristic analysis of dump truck unloading based on virtual prototyping. In *2011 IEEE/CSAE international conference on computer science & automation engineering* (pp. 697–700). IEEE. <https://doi.org/10.1109/CSAE.2011.5953312>
- Jiang, R. C., Liu, D. W., Wang, Z. C., & Fan, W. (2012). Dynamic characteristics simulation for lifting mechanism of dump truck based on virtual prototype. *Applied Mechanics and Materials*, 195–196, 754–757. <https://doi.org/10.4028/www.scientific.net/amm.195-196.754>
- Khan, A. A., & Rapal, N. (2006). Fuzzy PID controller: design, tuning and comparison with conventional PID controller. In *2006 IEEE/ICEIS international conference on engineering of intelligent systems* (pp. 1–6). IEEE. <https://doi.org/10.1109/ICEIS.2006.1703213>
- Kong, M. B., Li, W. P., & Tao, J. J. (2015). Fuzzy-PID control of hydro-pneumatic suspension for mining truck. *Computer Simulation*, 32(11), 169–173.
- Li, G., & Wang, T. (2013). The development of an auxiliary unloading device for dump trucks. In: SAE-China, FISITA (eds) *Proceedings of the FISITA 2012 world automotive congress. lecture notes in electrical engineering*, 196. Springer, Berlin, Heidelberg. https://doi.org/10.1007/978-3-642-33738-3_76
- Li, H. J., Li, R. F., Liu, J., & Lin, B. Q. (2017). Stability analysis of heavy duty tipper lifting operation based on ADAMS secondary development. *Agricultural Equipment and Vehicle Engineering*, 55(9), 10–14. <https://doi.org/10.3969/j.issn.1673-3142.2017.09.003>
- Li, W. P., Huang, Z. H., Cao, H. L., & Tao, J. J. (2017). Nonlinear control methods of active hydro-pneumatic suspension for mining dumping truck. *Computer Engineering and Applications*, 53(5), 222–226. <https://doi.org/10.3778/j.issn.1002-8331.1507-0086>
- Lin, J., & Lian, R. J. (2008). DSP-based self-organising fuzzy controller for active suspension systems. *Vehicle System Dynamics*, 46(12), 1123–1139. <https://doi.org/10.1080/00423110701809226>
- Mustafa, G. I. Y., Wang, H., & Tian, Y. (2019). Vibration control of an active vehicle suspension systems using optimized model-free fuzzy logic controller based on time delay estimation. *Advances in Engineering Software*, 127, 141–149. <https://doi.org/10.1016/j.advengsoft.2018.04.009>
- Si, J. P., Wang, G. S., & Ding, X. L. (2012). Analysis of dump truck unloading condition based on ANSYS. *Advanced Materials Research*, 548, 724–729. <https://doi.org/10.4028/www.scientific.net/amr.548.724>
- Tang, H. P., Zeng, L., Wang, S. Z., & Chen, H. S. (2018). Design of roll-over protective structure for heavy mining dumper based on topology optimization. *Chinese Journal of Engineering Design*, 25, 295–301. <https://doi.org/10.3785/j.issn.1006-754X.2018.03.007>
- Tian, Y. G., Zhao, J., & Wu, S. X. (2010). Analysis of dump truck rollover. *Auto Sci-Tech*, 6, 54–57. <https://doi.org/10.3969/j.issn.1005-2550.2010.06.014>
- Valladares, D., Carrera, M., Miralbes, R., & Castejon, L. (2014). Analysis of the torsional rigidity of a dump semi-trailer under unfavourable load conditions. *International Journal of Vehicle Design*, 64(2), 304–324. <https://doi.org/10.1504/IJVD.2014.058488>
- Valladares, D., Malon, H., Castejón, L., & Viñuales, A. (2013). Numerical-experimental analysis of the static roll stability of a demonstrator for the development of a rollover prevention device for dump semi-trailers. *International Journal of Vehicle Systems Modelling and Testing*, 8(2), 157–178. <https://doi.org/10.1504/IJVSMT.2013.054479>
- Wang, G. S., Si, J. P., Chen, Y. Y., Guo, L. N., & Zhao, Y. N. (2012). Structural stability analysis of dump truck body based on ANSYS. *Advanced Materials Research*, 588–589, 217–221. <https://doi.org/10.4028/www.scientific.net/amr.588-589.217>
- Wei, X. L., Cui, C. K., Liu, J., & Lin, B. Q. (2017). Design of anti-rollover warning system for dump truck in lifting operation. *Beijing Automotive Engineering*, 3, 10–13. <https://doi.org/10.14175/j.issn.1002-4581.2017.03.003>
- Xiao, L. J., Wang, M., Zhang, B. J., & Zhong, Z. H. (2020). Vehicle roll stability control with active roll-resistant electro-hydraulic suspension. *Frontiers of Mechanical Engineering*, 15(1), 43–54. <https://doi.org/10.1007/s11465-019-0547-9>
- Yao, W. J. (2016). Development of design system for simulation and optimization for lifting stability of dump trucks. Dissertation, Hefei University of Technology.
- Yu, H., Güvenç, L., & Özgüner, Ü. (2008). Heavy duty vehicle rollover detection and active roll control. *Vehicle System Dynamics*, 46(6), 451–470. <https://doi.org/10.1080/00423110701477529>

Publisher's Note Springer Nature remains neutral with regard to jurisdictional claims in published maps and institutional affiliations.